STORING ELASTIC ENERGY IN CARBON NANOTUBES

Frances Hill[1], Timothy Havel [2], A. John Hart [3], Carol Livermore[1]

[1] Department of Mechanical Engineering, MIT, Cambridge, MA, United States
[2] Engineering Systems Division, MIT, Cambridge, MA, United States
[3] Department of Mechanical Engineering, University of Michigan, Ann Arbor, MI, United States

Abstract: The potential performance of carbon nanotubes (CNTs) as springs for elastic energy storage is evaluated. Models are used to determine an upper bound on the energy density that can be reached in defect-free individual CNTs and in assemblies of such CNTs. Millimeter-scale CNT springs are constructed using 3 mm tall forests of multi-walled CNTs as the starting material, and tensile tests are performed to measure the s rings' sti ness, strength and elastic ro erties The highest recorded values for specific strength and specific stiffness are 0.7 N/tex and 21 N/tex, respectively. The measured strain energy density of these continuous CNT fibers is equivalent to the energy density of steel springs.

Key words: Carbon nanotubes, fibers, energy storage, energy density, mechanical springs

1. INTRODUCTION

A new approach to storing energy in carbon nanotubes (CNTs) is presented, along with its calculated performance and initial experimental results. In this approach, an ordered grouping of carbon nanotubes (CNTs) is used as a spring to store energy for later use, much as a steel spring stores energy in a mechanical watch. The CNT spring differs from a conventional steel spring in the exceptional material properties that its CNT composition offers. The mechanical properties of CNTs include a high effective oung's odulus o ca. 1 TPa and experimentally demonstrated elastic strains as high as 6% [1], with theoretically predicted strains as high as 20% [2] in the absence of defects. Together, these properties offer the potential for elastic energy storage systems at energy densities that are three orders of magnitude higher than those of conventional steel springs, and indeed comparable to lithium-ion batteries.

At the molecular scale, CNTs can function as mechanical springs that store a great deal of energy for their size due to their networks of strong, carbon-carbon bonds. The challenge remains to build springs that store macroscopically significant amounts of energy in large arrays of nanotubes and recover the energy in a controlled fashion. In this paper, we first present models of energy storage in CNTs to determine the theoretical upper bound on the elastic energy that may be stored in CNTs, and the optimal mode of deformation for energy storage. Next, we summarize the results of experimental tests performed on a first generation of springs to examine the performance of CNT groupings as mechanical springs.

2. ENERGY STORAGE MODELING

The energy density that can be stored in a CNT under a load is estimated by treating a CNT as a hollow, cylindrical beam and assigning a thickness of 0.34 nm to each CNT shell based on the continuum assumption [3 he co only e loyed oung's modulus of 1 TPa is employed. For a CNT loaded in tension or compression, the energy density is

$$u \quad \frac{1}{2} E \varepsilon^2 k \tag{1}$$

where E is the oung's odulus, is the applied strain, and k is a factor to account for the unfilled space at the center of a CNT and/or the volume fraction of CNTs within groupings. In tension, the maximum strain that can be applied is limited only by the elastic limit. In compression, the maximum applied strain is limited by either the elastic limit or the buckling limit, whichever is reached first. In bending, the maximum energy density of a CNT is

$$u \quad \frac{1}{8} E \varepsilon_{\max}^{\ 2} \ 1 \quad \frac{r_i}{r_o}^4 \quad k \tag{2}$$

where r_i and r_o are the inner and outer radii of the continuum cylinder, $_{max}$ is the maximum applied strain at which either the elastic limit is reached or buckling occurs, and k accounts for the volume fraction of CNTs in a grouping. Finally, in torsion the maximum energy density in a CNT is

$$u \quad \frac{M_{cr}^{\ 2}}{2GJ \ r_o^2} k \tag{3}$$

where G is the shear modulus, $J \ \frac{}{2}(r_o^4 \ r_i^4)$ is the polar moment of inertia of the beam, and M_{cr} is the

maximum moment that can be applied before reaching the elastic limit or the onset of buckling.

Analysis of Eqs. 1-3 for single-walled (SWCNTs) and multi-walled CNTs (MWCNTs) with different diameters and number of shells reveals that in bending, compression and torsion, higher energy densities can be reached in SWCNTs than in MWCNTs because of their higher buckling strains [4] and greater radial stability [5]. In tension, SWCNTs are favored over MWCNTs because of the difficulty of grasping and loading MWCNT inner shells [6].

The maximum strain energy density of SWCNTs is plotted as a function of diameter in Fig. 1 for four deformation modes. The energy density in mechanically deformed SWCNTs is highest under tensile loading as long as elastic strains greater than 9% can be reached. Assuming maximum elastic strains of 15%, the energy density in CNT springs is predicted to be three orders of magnitude greater than the maximum energy density of steel springs and eight times greater than the energy density of lithium-ion batteries.

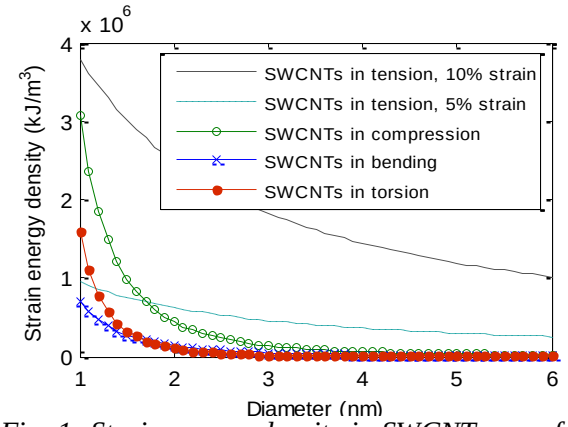

Fig. 1: Strain energy density in SWCNTs as a function of diameter for different deformation modes.

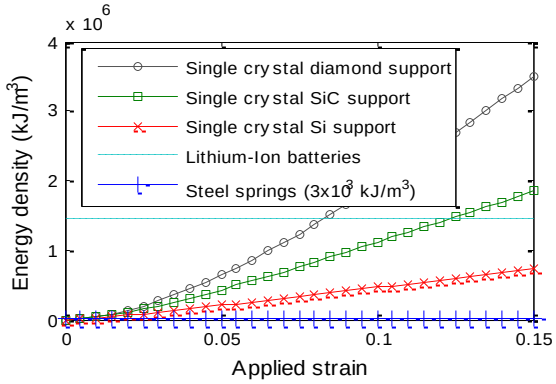

Fig. 2: Energy density of SWCNTs bundles under tensile loading with support structures made of single crystal diamond, silicon and silicon carbide.

Models were also generated of a more complete system, to represent a power source that includes not only a CNT spring but also hardware to hold the stretched spring in place prior to discharge and optionally control the rate of energy release from the spring [4]. Fig. 2 plots the predicted energy density of a system that includes a support structure and a spring, and shows a maximum achievable overall stored energy density that is comparable to lithium-ion batteries. Even once a support structure is considered, a CNT spring stores energy with a density more than two orders of magnitude higher than a steel spring and on the same level as batteries.

3. MECHANICAL PROPERTIES OF FIBERS

Fibers of continuous MWCNTs were fabricated to study their mechanical properties and energy storage capabilities. These milliscale CNT springs were constructed from 3 mm tall forests of MWCNTs (Fig. 3). Each spring was created by removing a small fiber from the edge of a forest. Additional springs were constructed from 1.2 mm tall pillars with 200 µm by 200 µm cross-sections. Both the pillars and forests are made of MWCNTs with an average of 4-5 shells and mean outer diameters of 10 nm. The areal density of the forests is 2-2.5 x 10^{14} MWCNTs/m^2, corresponding to a mass density of 0.015-0.019 g/cm^3.

A range of techniques were tested for creating compact, ordered, interacting groupings of CNTs from the starting forest material, including compaction by mechanical pressure and capillary-driven densification [7] using hexane, toluene and benzene. Capillary-driven densification increased the initial density of the fibers by a factor of 7, while mechanical compression increased the density by a variable factor as high as 16. Both densification techniques resulted in densities far below the upper limiting density of graphite. The densified fibers were secured to a frame using epoxy, and tensile tests were performed on the springs to measure their stiffness, strength, and elastic properties.

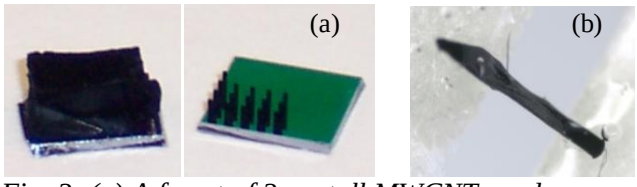

Fig. 3: (a) A forest of 3mm tall MWCNTs and an array of 1.2mm tall pillars (b) Fiber in a loading frame.

The fibers were loaded in tension up until failure to obtain stress-strain curves. From these tests, one can calculate both stress within the fiber (using the outer cross-sectional area of the densified fiber) as well as the stress in the CNTs (using the effective loading area of the CNT shells within the fibers, estimated from the volume fraction of the as-grown forests). A typical stress-strain curve is shown in Fig. 4, exhibiting a

linear relation between stress and strain. The maximum strength and stiffness of the fibers obtained to date are 70 MPa and 1.7 GPa, and the maximum measured strength and stiffness just considering the CNT area obtained to date are 1.6 GPa and 45 GPa, respectively. The conservative assumption is made that all shells within the MWCNTs are supporting loads; if it is assumed that only the outer shells support the load, the highest strength and stiffness just considering the CNT area become 2.8 GPa and 89 GPa. The strain at failure for the fibers was variable and ranged between 1% and 20%. Failure of the fibers tends to occur as a single unit, with the fracture zone tending to be a clean cut across the fiber; this indicates that there are interactions between CNTs throughout the cross-section of the fiber.

Data for fiber strength and CNT strength are plotted as a function of uncompressed fiber cross-sectional area in Fig. 5. The plots reveal that higher strengths were measured in smaller fibers. The same trend was observed between modulus and area, with the highest fiber and CNT moduli measured in fibers with the smallest cross-sectional areas. These results may be an indication of uneven tensile loading within the fibers, which would concentrate the load to particular regions within the fiber and produce lower than expected failure loads. As a result, higher fiber strength and stiffness, as well as more accurate CNT strength and stiffness, are recorded in smaller fibers, where uniform loading is more achievable. Uneven loading may be the result of the epoxy grips or non-uniformities in the fibers due to the densification process. The large spread in the strength and stiffness data can likely be attributed to uneven loading, though uncertainties in the density of the forests may also have been a contributing factor.

The results are further summarized in Fig. 6, which plots the specific stress vs. specific stiffness. The highest recorded specific strength and stiffness are 0.73 N/tex and 21.5 N/tex. While encouraging, these preliminary results fall below the highest values obtained for fibers to date by direct spinning from the gaseous phase [8]. This is not surprising given that the starting material in the spinning technique is made of high-quality, high temperature grown single- and double-walled CNTs rather than the lower temperature, 4-shell MWCNTs forests used here. The fact that the strength reported here is as high as it is indicates the strength-inducing advantages of the fiber assembly approach based on forests as the starting material.

Cyclic loading tests (Fig. 7) performed on the fibers provide additional insight into the mechanisms taking place within the fiber during tensile loading. The loading behaviour changes after the first loading cycle but remains consistent following the second cycle. These subsequent load-unload curves display an increased modulus, once slack has been removed, as well as hysteretic behaviour. This presumably arises because the CNTs grown in the forests are not straight and perfectly aligned, but exhibit bending and kinks. The first loading cycle loads the fiber while taking up the slack, while subsequent loading cycles simply load the fiber once slack has been removed. These results indicate considerable disorder at the micro/nanoscale.

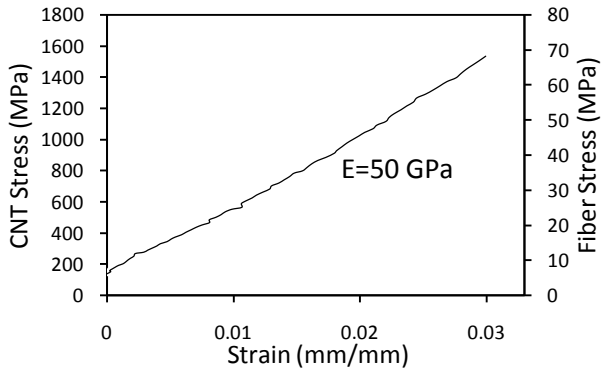

Fig. 4: CNT stress and fiber stress vs. strain for a typical fiber loaded in tension up to failure.

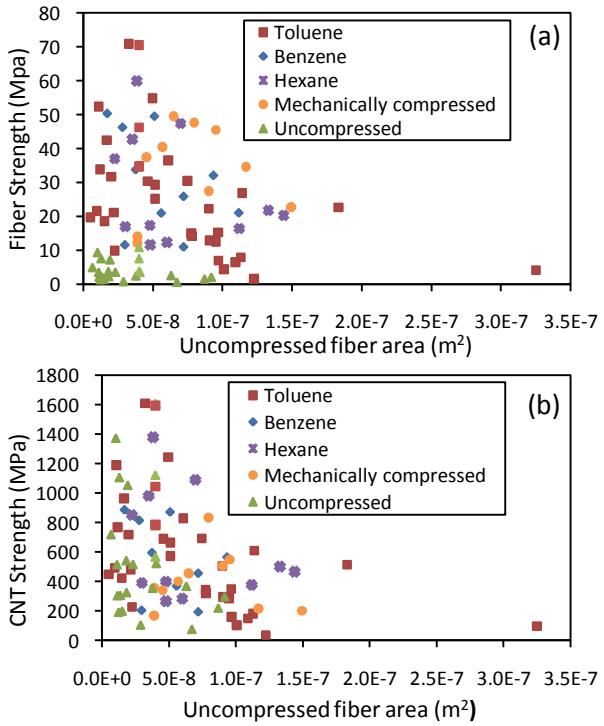

Fig. 5. (a) Fiber strength and (b) CNT strength plotted as a function of uncompressed fiber area.

The strain energy density stored in a fiber under a load is

$$u = \int_0^{\varepsilon} \sigma(\varepsilon) d\varepsilon \qquad (4)$$

This energy density calculation is applied only to loading cycles after an initial load-unload cycle (corresponding to cycle 2 through 5 in Fig. 7) once the

slack in the fiber is taken up. The maximum recoverable energy recorded to date is 2×10^3 kJ/m^3 or 15 kJ/kg, which is comparable to the energy density by volume and greater than the energy density by mass of steel springs. The energy density by volume remains three orders of magnitude lower than the theoretically predicted maximum energy density, and provides a lower bound on what could be achieved in more advanced implementations of CNT springs.

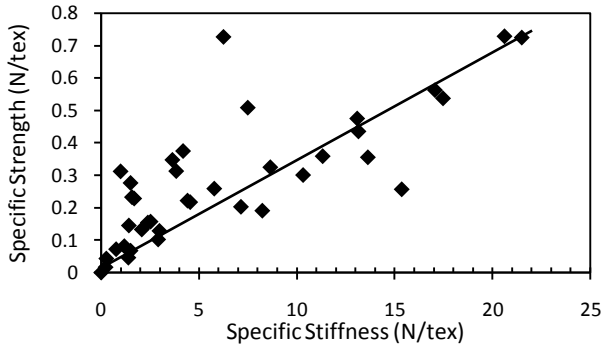

Fig. 6: Specific stiffness plotted against specific strength for fibers densified using capillary forces.

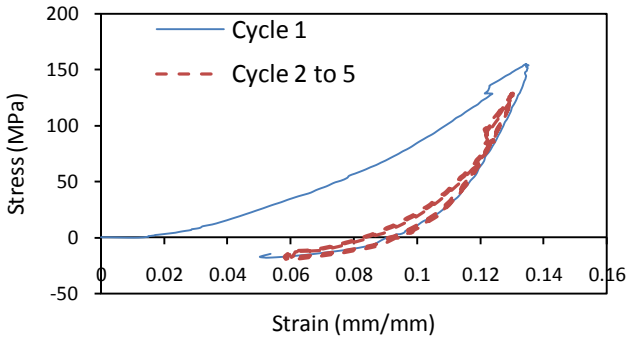

Fig. 7: Cyclic loading of a fiber.

4. CONCLUSION

Models of CNTs under a mechanical load show that the theoretical upper limit on energy density that can be reached in CNTs employed as springs can match the energy density of electrochemical batteries, even once additional hardware such as a support structure is taken into consideration. This result has motivated the fabrication of CNT fibers to serve as mechanical springs.

The current work on fibers demonstrates that building fibers with excellent mechanical properties using forests as a starting material shows significant potential. Given that the forests used here are made of lower-quality MWCNTs, the specific strength and stiffness of the fibers compare well to state of the art fibers produced by high-temperature spinning processes.

Additional work is still needed to increase the strength and stiffness of these fibers. In particular, improved densification techniques are necessary to create higher density fibers that are able to support loads uniformly. Techniques to straighten the CNTs and improve the internal organization within the forests are still needed to produce fibers that exhibit elastic behaviour and can act as elastic springs. The current energy density that was stored and subsequently released from this first-generation of fibers already matches the energy density of steel springs, but still remains three orders of magnitude below the maximum predicted theoretical energy density of CNT springs.

ACKNOWLEDGEMENTS

The authors would like to thank Eric Meshot, Sameh Tawfick, Jonathan Leavitt and Lori Pressman for their valuable contributions, and NSERC and the Deshpande Center for Technological Innovation for their financial support of this work.

REFERENCES

[1] Walters D A, Ericson L M, Casavant M J, Liu J, Colbert D T, Smith K A, Smalley R E 1999 Elastic strain of freely suspended single-wall carbon nanotube ropes. *Applied Physics Letters.* **74** 3803-3805

[2] Liew K M, Hea X Q, Wong C H 2004 On the study of elastic and plastic properties of multi-walled carbon nanotubes under axial tension using molecular dynamics simulation *Acta Materialia.* **52** 2521-2527

[3] Salvetat J, Bhattacharyya S, Pipes R B 2006 Progress on mechanics of carbon nanotubes and derived materials *Journal of Nanoscience and Nanotechnology.* **6** 1857-1882

[4] Hill F A 2008 Energy Storage in Carbon Nanotube Super-Springs *S.M. Thesis, Massachusetts Institute of Technology.*

[5] Pantano A, Parks D M, Boyce M C 2004 Mechanics of deformation of single- and multi-wall carbon nanotubes *Journal of the Mechanics and Physics of Solids*. **52** 789-821

[6] Qian D, Liu W K, Ruoff R S 2003 Load transfer mechanism in carbon nanotube ropes *Composites Science and Technology.* **63** 1561-1569

[7] Chakrapani N, Wei B, Carrillo A, Ajayan P M, Kane R S 2004 Capillarity-driven assembly of two-dimensional cellular carbon nanotube foams *PNAS* **101** 4009-4012

[8] Koziol K, Vilatela J, Moisala A, Motta M, Cunniff P, Sennett M, Windle A 2007 High-Performance Carbon Nanotube Fiber *Science*. **318** 1892-1895